

Modeling and Analysis of the W7-X High Heat-Flux Divertor Scraper Element

A. Lumsdaine¹, J. Boscary², E. Clark³, K. Ekici³, J. Harris¹, D. McGinnis¹, J.D. Lore¹, A. Peacock², J. Tipton⁴, and J. Tretter²

¹Oak Ridge National Laboratory, Oak Ridge, TN USA

²Max Planck Institute for Plasma Physics, EURATOM Association, Garching, Germany

³University of Tennessee, Knoxville, TN USA

⁴University of Evansville, Evansville, IN USA

Corresponding author e-mail: lumsdainea@ornl.gov

Abstract—The Wendelstein 7-X stellarator experiment is scheduled for the completion of device commissioning and the start of first plasma in 2015. At the completion of the first two operational phases, the inertially cooled test divertor unit will be replaced with an actively cooled high heat-flux divertor which will enable the device to increase its pulse length to steady-state plasma performance. Plasma simulations show that the evolution of bootstrap current in certain plasma scenarios produce excessive heat fluxes on the edge of the divertor targets. It is proposed to place an additional “scraper element” in the ten divertor locations to intercept some of the plasma flux and reduce the heat load on these divertor edge elements. Each scraper element may experience a 500 kW steady-state power load, with localized heat fluxes as high as 20 MW/m². Computational analysis has been performed in order to examine the thermal integrity of the scraper element. The peak temperature in the CFC, the total pressure drop in the cooling water, and the increase in water temperature must all be examined to stay within specific design limits. Computational fluid dynamics (CFD) modeling is performed to examine the flow paths through the multiple monoblock fingers as well as the thermal transfer through the monoblock swirl tube channels.

Keywords—Wendelstein 7-X; Stellarator; Divertor; Heat flux

I. INTRODUCTION

The Wendelstein 7-X stellarator experiment is scheduled to complete construction and begin operation in 2015. After the first two operational phases, the inertially cooled test divertor unit will be replaced with an actively cooled high heat-flux divertor which will enable the device to increase its pulse length and its steady-state plasma performance. For this phase of machine operation, plasma simulations show that the evolution of bootstrap current in certain plasma scenarios produce excessive heat fluxes on the divertor edge elements. (For details on the high heat-flux divertor, its design and cooling, see [1-3]). Simulations have shown the heat fluxes on these edge elements to be significantly above the design limit of 5 MW/m². It is proposed to place an additional “scraper element” in the ten divertor locations that will capture some of

This manuscript has been authored by UT-Battelle, LLC, under Contract No. DE-AC05-00OR22725 with the U.S. Department of Energy. The United States Government retains and the publisher, by accepting the article for publication, acknowledges that the United States Government retains a non-exclusive, paid-up, irrevocable, world-wide license to publish or reproduce the published form of this manuscript, or allow others to do so, for United States Government purposes.

the plasma flux and reduce the heat load on these divertor edge elements. Two views of the scraper element are shown in Figs. 1 and 2.

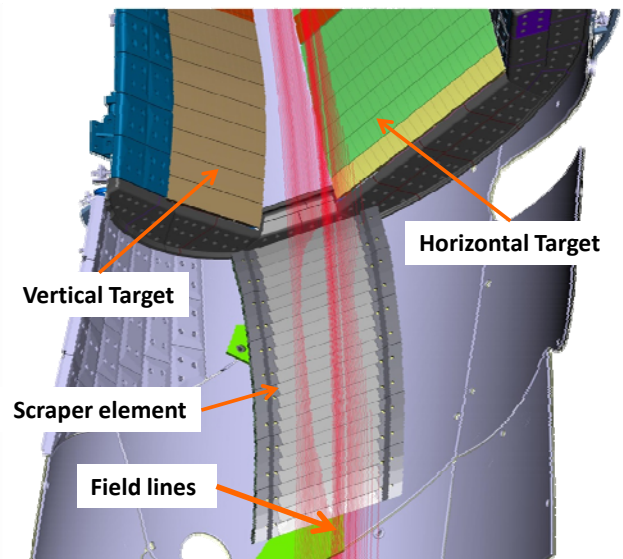


Fig. 1 Top view of scraper element

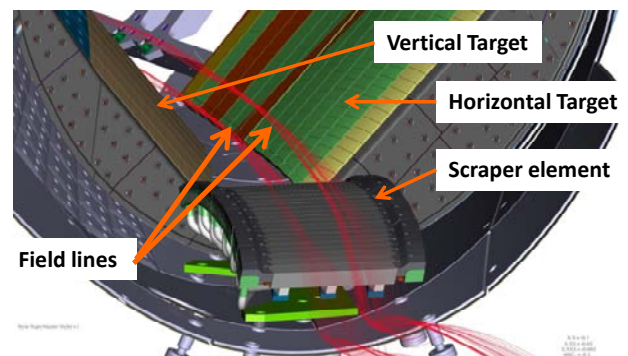


Fig. 2 Front view of scraper element

The scraper element may experience a 500 kW steady-state power load, with localized heat fluxes as high as 20 MW/m².

It will be constructed using carbon-carbon fiber composite (CFC) monoblock technology (see Fig. 3), and placed between the existing in-vessel components (IVCs) and the plasma volume in an extremely limited space. CFC monoblocks designed for ITER have been qualified to survive 20 MW/m² heat flux [4-6]. The convective heat fluxes on the divertor components have been modeled using magnetic field configurations where the contribution due to equilibrium plasma currents has been included [7]. The scraper element surface was then designed iteratively through an integrated computer-aided design and thermal analysis process. The design of the scraper element structural support, hydraulic paths, and thermal protection involved numerous trade-offs due to the extreme thermal environment and severely limited space.

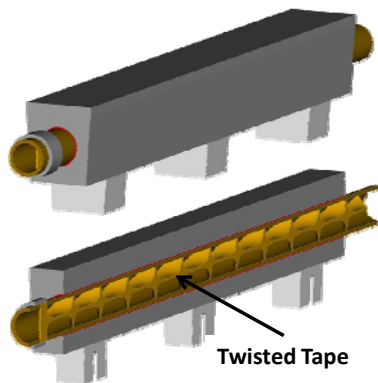


Fig. 3 CFC monoblock finger (and side cross-section)

Computational modeling has also been performed in order to model the thermal and structural integrity of the scraper element. The peak temperature in the CFC, the total pressure drop in the cooling water, and the increase in water temperature must all be examined to stay within specific design limits. Computational fluid dynamics (CFD) modeling is performed to examine the flow paths through the multiple monoblock swirl tube channels. Finite element analysis is integrated into the CFD results in order to ensure the structural integrity of the component.

II. SCRAPER ELEMENT DESIGN

A. Design Requirements

The following design requirements have been established for the scraper element:

1. Heat load reduction on end of divertor target element to less than 5 MW/m².
2. Design is as far as possible compatible with existing IVCs.
3. Design uses existing panel holders as fixation.
4. Design is compatible with existing manufacturing technology.
5. Heat load maintained below the technical limit of the monoblock technology (qualified to 20 MW/m² for ITER).
6. Pressure drop in cooling water from supply to return \leq 1.4 MPa, with return pressure of \geq 1.0 MPa.

7. Bulk water temperature \leq 80 °C (50 °C increase).
8. CFC surface \leq 1200 °C.
9. 6 mm of CFC should remain above the cooling tube (even after 3D surface machining).
10. The components must fit in entry port, be able to move into vessel from entry port.

In order to meet all of these requirements, it is necessary to integrate the function of physics modeling, computer-aided design, and computer-aided engineering. Physics modeling is used to evaluate whether requirements 1 and 5 are satisfied. Computer-aided design tools assist in ensuring that requirements 2, 3, 4, 9, and 10 are satisfied. And computer-aided engineering tools (such as CFD) are used to verify that requirements 6, 7, and 8 are satisfied. Meeting all of these requirements is an iterative process involving close communication between the physics, design, and engineering functions.

B. Evolution of the Scraper Element

The integrated nature of the scraper element design process can be seen by examining the iterations of the scraper element that have led to the current feasible design. One issue that needed to be resolved was the direction of the cooling fingers, whether these should run toroidally (in the long direction) or poloidally (in the short direction). Previous analyses indicated that in order to meet the pressure drop, peak CFC temperature, and water temperature requirements, the cooling fingers need to be oriented poloidally [8].

Since the primary purpose of the scraper element is to protect the edges of the divertor target, the scraper element must be designed from the top down. That is, first the geometry of the top surface must be defined, and then analyzed to confirm that the heat flux on the divertor target ends do not exceed 5 MW/m² (design requirement 1) and the heat flux on the scraper element itself does not exceed 20 MW/m² (design requirement 5). Fig. 4 shows the designs of five scraper element surfaces, where the horizontal target is at the top of each figure, the vertical target is at the bottom of each figure, and the scraper element is to the right. Magnetic field line strike points (which are modeled to carry convective heat flux) are shown as red or blue dots in each model.

Fig. 4(a) is an initial concept for the scraper element, which lies in the pumping gap. This would cause too great a restriction on the pumping of neutrals. This design is also too geometrically complex for engineering design, and too close to the divertor targets to allow space for cooling. In Fig. 4(b), the scraper element is moved out of the pumping gap. But this design has significant curvature (poloidally), and would be difficult to provide adequate cooling. Additionally, it would be difficult to supply cooling to the small region that remains over the pumping gap. The scraper element design shown in Fig. 4(c) also is too close to the divertor targets to provide cooling, and is too geometrically complex in this area for a cost-effective design. Fig. 4(d) is completely out of the pumping gap, but interferes with the machine's protective panels (not shown) once the cooling pipes are included. Fig. 4(e) is similar to Fig. 4(d), but shorter, using 24 monoblock fingers instead of 32. This not only allows the scraper element to better fit into

the extremely constrained space inside the W7-X vessel, it is also cost effective, with 25% fewer monoblock fingers.

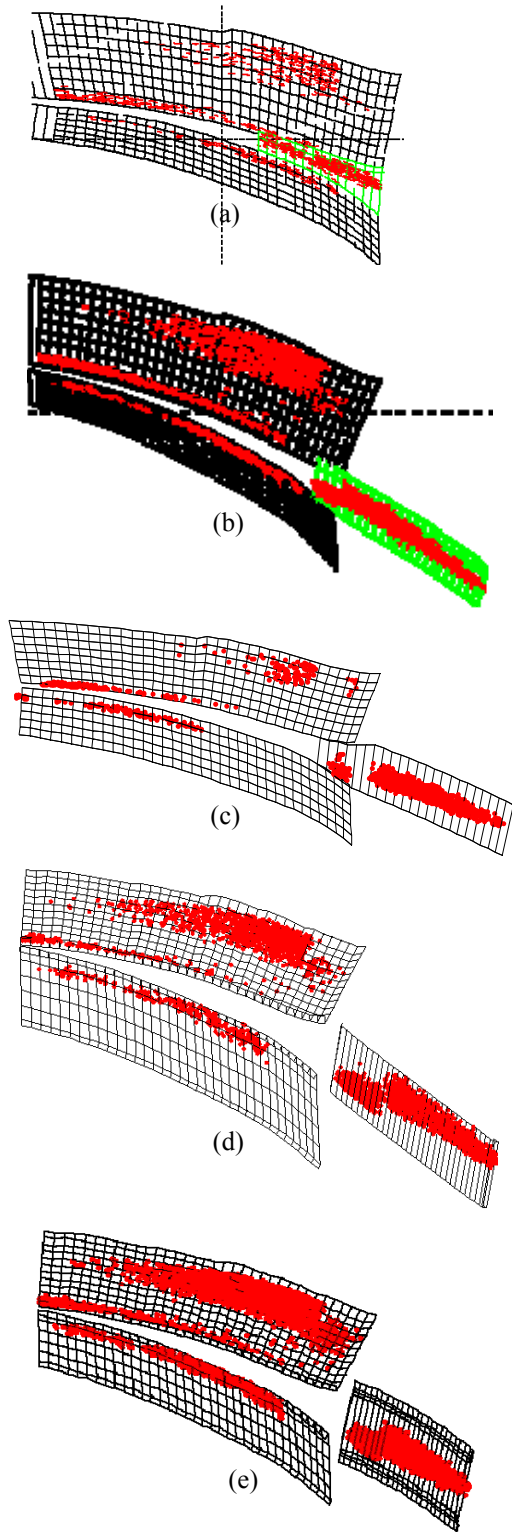


Fig. 4 Evolution of scraper element

III. THERMAL FLUID ANALYSIS

In order to ensure that the scraper element design meets the requirements outlined in the previous section, thermal-fluid analyses are performed. The primary concern is to meet the requirements on the maximum pressure drop, the maximum bulk water temperature, and the maximum CFC surface temperature. First, analytic and empirical relationships are used to perform hydraulic analysis. This is then confirmed with computational fluid dynamics (CFD) calculations. Finally, a CFD thermal analysis is performed.

A. Hydraulic Calculations – Analytical and Empirical

The axial water flow velocity for previous qualifications of CFC monoblocks was between 10 m/s and 12 m/s, so it assumed that this will be necessary for the current design to meet the requirement of handling 20 MW/m² steady-state heat flux. It is assumed that the W7-X project will be able to provide between 20 m³/hr and 30 m³/hr volume flow rate of water to each scraper element. The first question to answer is, how many parallel fluid circuits (or “modules”) should the water run through (eight circuits of three fingers each, six circuits of four fingers each, four circuits of six fingers each, etc.)? If the water is divided 24 ways, each of the 24 monoblock fingers will have a very low pressure drop, but each will also have a very low water velocity. On the other hand, if the entire scraper element is a single module, with all of the water supply running from one finger to the next until it passes through all 24 fingers, then the water velocity will be very high, but the pressure drop will be well beyond what is defined in design requirement 6.

The cross-section of the CFC monoblock produced for the scraper element is shown in Fig. 5. The CuCrZr tube has a 12 mm inner diameter, with a 1 mm thickness, copper twisted tape insert (attached to the tube with a tab at one end). Fig. 6 shows the axial velocity of the cooling water in each monoblock tube versus the number of different flow channels (or “modules”) for different volume flow rates. (Note that the tube cross-section used to calculation the axial flow velocity subtracts out the area of the twisted tape). Based on a water velocity between 10 m/s and 12 m/s for the ITER-qualified CFC monoblocks, an 8 channel configuration looks marginally feasible. This would require at least 30 m³/hr, which would be difficult to provide in the existing water supply and feed pipe. A 6 channel configuration could produce an axial velocity of almost 12 m/s with a 26 m³/hr volume flow rate.

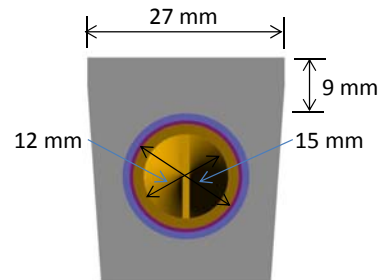


Fig. 5 Monoblock cross-section

Next, the pressure drop in various configurations is examined. For a tube with a twisted tape insert, the pressure drop may be calculated according to the correlations developed by Manglik and Bergles for turbulent flow [9]:

$$\Delta p = f \frac{l}{D} \frac{\rho u_m^2}{2} \quad (1)$$

where f is the friction factor, l is the length of the tube, D is the hydraulic diameter, ρ is the water density, and u_m is the mean water velocity. The friction factor is calculated using:

$$f = \frac{0.0791}{Re^{0.25}} \left[\frac{\pi}{\pi - 4(\delta/D)} \right]^{1.75} \left[\frac{\pi + 2 - 2(\delta/D)}{\pi - 4(\delta/D)} \right]^{1.25} \left[1 + \frac{2.752}{y^{1.29}} \left(\frac{\mu_{bulk}}{\mu_{wall}} \right)^{-0.25} \right] \quad (2)$$

where d is the thickness of the twisted tape, and y is the pitch of the twisted tape defined by:

$$y = \frac{L_{180^\circ \text{Turn}}}{D} \quad (3)$$

The pitch is chosen to be 2 for this application, as this has been shown to be effective for heat transfer for a variety of flow conditions [10]. The pressure drop of a 180 degree pipe bend (with no twisted tape insert) is calculated using [11]. Fig. 7 shows the pressure drop versus the number of flow channels for different volume flow rates. It can be seen that for the 6 channel configuration, the pressure drop is less than 700 kPa regardless of volume flow rate. However, this value is based on empirical relationships including a 180° pipe bend between monoblock fingers. It is necessary to perform a CFD analysis to confirm that this design is capable of meeting the requirement of a total pressure drop less than 1.4 MPa.

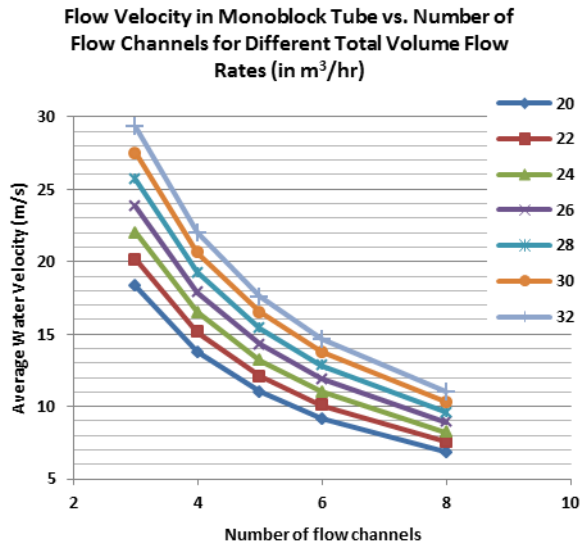


Fig. 6 Monoblock axial flow velocity

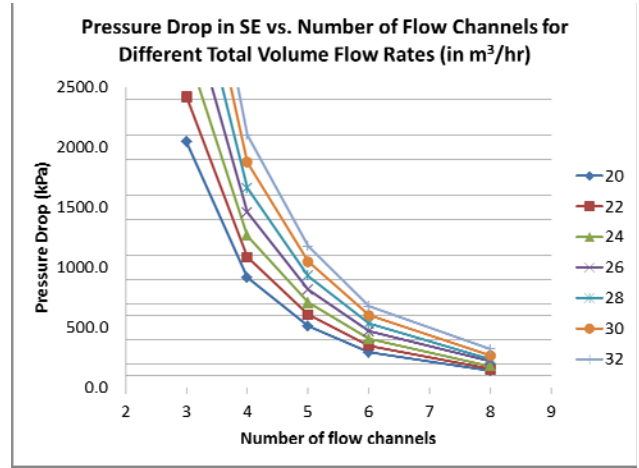


Fig. 7 Pressure drop per scraper element module

B. Hydraulic Calculations – Computational Fluid Dynamics

Based on the empirical results, a case where 6 parallel flow channels (of four fingers each) is examined, as shown in Fig. 8. Analysis is performed using the ANSYS CFX commercial package. Only one of the six modules is modeled, as shown in Fig. 9. Since this is a hydraulic (pressure and flow) analysis only, it is not necessary to model the CFC. The converged model (shown in Fig. 10) has a total of 927,535 nodes and 2,380,109 elements. A k-ε turbulence flow model is used to model the water flow. The inlet condition is the mass flow rate (which was varied to obtain several results). The outlet pressure is set at 1.4 MPa. (The saturation temperature at this pressure is 195 °C). Results are obtained for four different flow rates resulting from 20, 22, 24 and 26 m³/hr total water flow per scraper element.

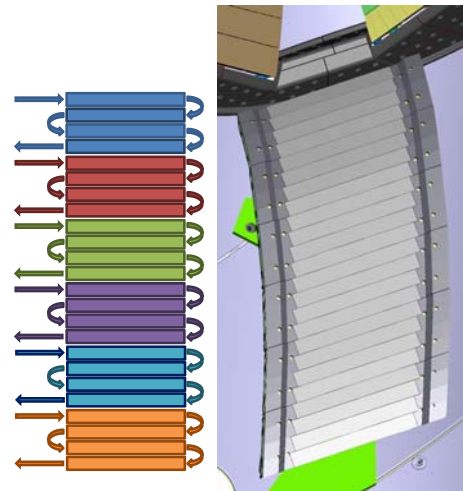


Fig. 8 Schematic of scraper element modules flow sequence

Pressure drop contours are shown in Fig. 11. The pressure drop results are shown in Table 1. It is noted that the CFD

results predict pressure drops about 50% higher than those calculated from empirical models. The primary source of difference is in the pipe connections. For the twisted tape regions, the CFD model computes about a 25% higher pressure drop than is calculated from the empirical model. But even with these higher calculated pressure drops, sufficient margin remains to meet the design criteria of 1.4 MPa maximum. It should be noted that this design requirement includes the pressure drop of the supply line to the scraper element, and the manifold with feeds all six scraper element modules, and these components are not modeled in this analysis. It is believed that these results show sufficient margin to meet the requirement once these components are included. Further analysis will be performed in the future to confirm this.

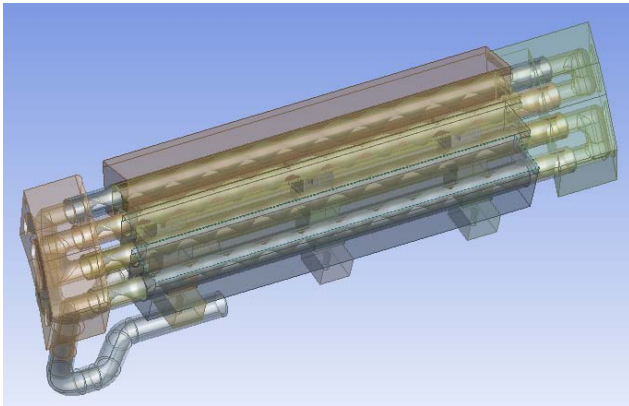


Fig. 9 Model of single four-finger scraper element module

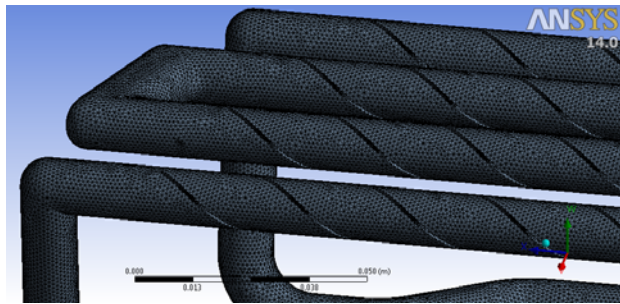


Fig. 10 Mesh of water for CFD

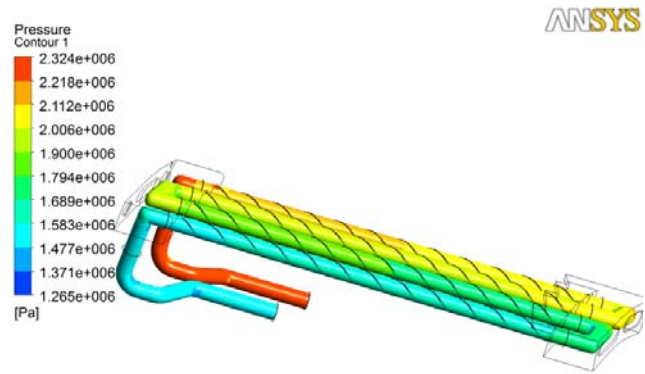


Fig. 11 Pressure contours for scraper element module

TABLE I. CFD PRESSURE DROP RESULTS

Inlet Volume Flow Rate (m ³ /hr)	Axial Flow Velocity (m/s)	Actual Flow Velocity (m/s)	Calculated Pressure Drop (kPa)	CFX Pressure Drop (kPa)
20	9.19	11.64	333	484
22	10.08	12.81	393	578
24	10.99	13.98	458	684
26	11.91	15.14	528	789

C. Thermal Calculations

In order to confirm that the CFC peak temperature remains below 1200°C (design requirement 8), ANSYS CFX is used to perform a thermal analysis on a single monoblock finger. The following assumptions and boundary conditions are included in the model:

- K-ε turbulence model using wall functions ($y^+ \approx 100$)
- Constant water properties
- Single phase flow
- Materials:
 - CFC has orthotropic thermal conductivity (300 W/m²-K through vertical axis; 100 W/m²-K through other axes [12])
 - Pipe is CuCrZr
 - Twisted tape is copper
- CFC has perfect thermal contact with pipe, twisted tape has no thermal contact with pipe
- Smooth, no slip walls
- Inlet
 - Temperature = 30°C
 - Velocity = 10 m/s (assuming 22 m³/hr volume flow rate)
- Outlet
 - Zero normal gradients
 - Average static pressure = 0 Pa

To gain confidence in the simulation, the fluid domain model was validated against published semi-empirical

correlations for single-phase twisted-tape enhanced heat transfer in uniformly heated pipes [9]. The desired mesh with $y^+ \approx 100$ was refined twice. Figure 12 shows the comparative results. Asymptotic convergence is not yet achieved, however, the simulation falls within the reported data spread of 10% and results are conservative.

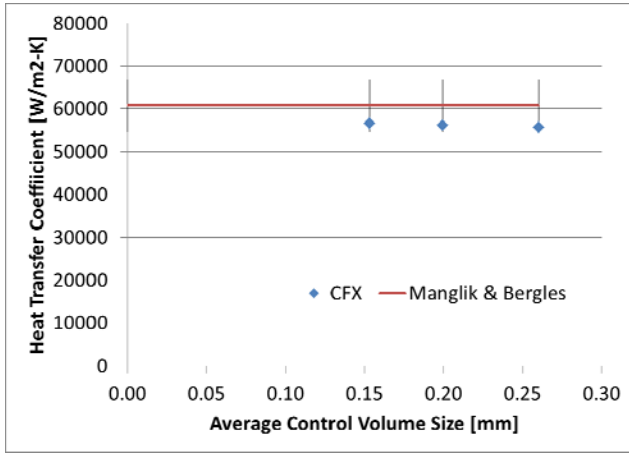


Fig. 12 Heat application in ANSYS CFX

The worst-case heat load is applied to the CFC surface. Results from the DIV3D code [7] are examined to identify the monoblock finger that has the highest total heat. Fig. 13 shows the DIV3D results, indicating the heat fluxes mapped onto the scraper element surface. The highest total heat is on a finger near the center of the scraper element, with 34.4 kW deposited. The heat flux across the finger is given in Table II, and this heat flux is shown graphically on the CFD model in Fig. 14.

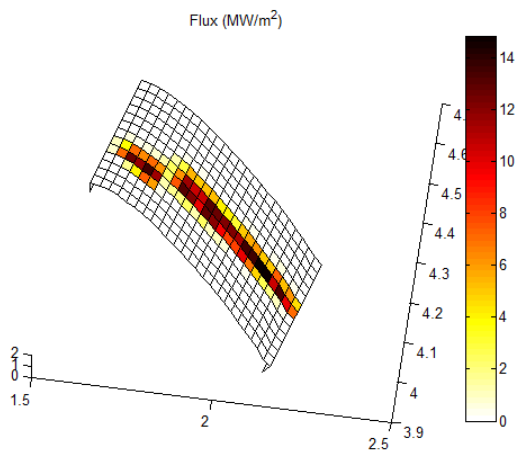


Fig. 13 DIV3D result – heat flux on scraper element

TABLE II. HEAT FLUX FOR MONOBLOCK FINGER 9 (MW/M²)

Poloidal index	1	2	3	4	5	6	7	8
	0.00	0.77	8.89	16.75	10.18	3.74	0.00	0.00

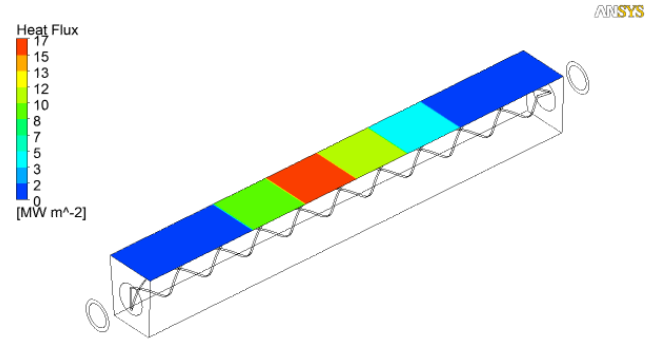


Fig. 14 Heat flux boundary condition application in ANSYS CFX

The simulation is run until the mean residuals have dropped by at least 3 orders of magnitude. The converged model has 1,994,782 nodes. Results are shown in Fig. 15-17. The maximum CFC temperature is shown to be 1208°C which is essentially at the design criteria limit (CFC surface ≤ 1200 °C). It should be noted that the water temperature solution indicates localized nucleate boiling will take place. This will increase heat transfer performance and is not included in the simulation.

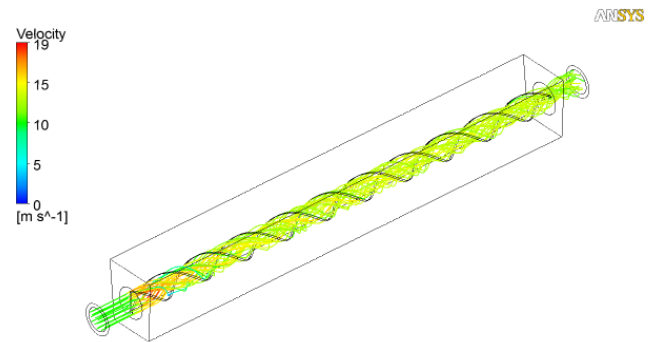


Fig. 15 Flowlines from CFD result

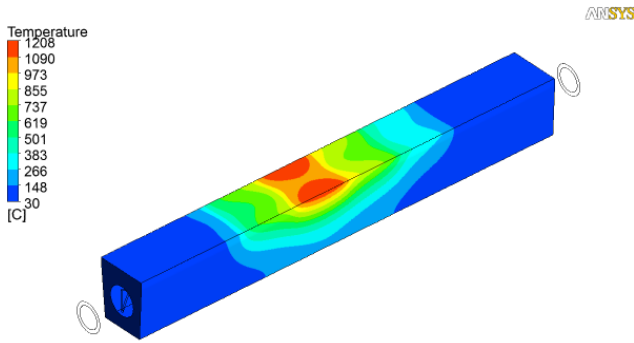


Fig. 16 CFC temperature from CFD result

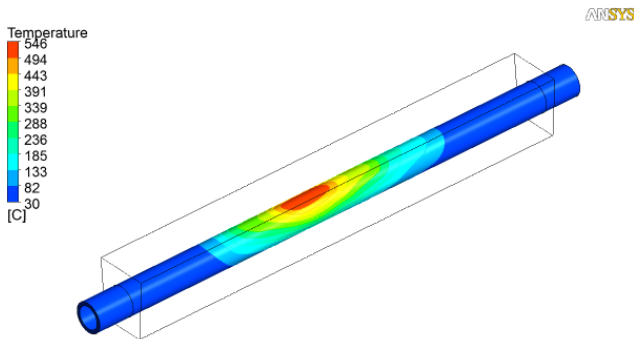


Fig. 17 CuCrZr tube temperature from CFD result

IV. CONCLUSION

An initial design for the Wendelstein 7-X high heat-flux scraper element surface has been analyzed, integrating the tools of computer-aided design, computational physics, and engineering analysis. Next steps in evaluating and completing the design are as follows.

- A more detailed CFD model and FE model will be analyzed, as detailed in the section above.
- Thermal analysis will be performed for an entire scraper element module.
- Hydraulic analysis will be performed for the entire scraper element, in order to confirm flow balance in the different modules.
- Parametric study will be conducted to calculate heat flux on the scraper element surface if the scraper element is located at the limits of the assembly tolerance within the device.
- The radiation heat load (calculated to be about 100 kW/m^2 on most of the scraper element surface) will be included in the model.
- Critical heat flux (CHF) criteria will be examined and compared to computed heat flux on the cooling water.

- Structural analysis will be performed on entire scraper element modules, as well as on the scraper element support structure.
- An uncooled “test” scraper element will be built to place in W7-X during the first phase of plasma operation in order to determine the actual heat loads experience during operation.
- A prototype scraper element module will be built and tested in realistic heat flux conditions (such as was done in [13]).

ACKNOWLEDGMENT

This work is supported by the US Department of Energy, Contract DE-AC05-00OR22725.

REFERENCES

- [1] A. Peacock, J. Boscary, M. Czerwinski, G. Ehrke, H. Greuner, P. Junghanns, et al, “Wendelstein 7-X high heat flux components,” Proceedings of the 2013 Symposium on Fusion Engineering, San Francisco, CA, 2013.
- [2] B. Medevitch, A. Vorköper, J. Boscary, A. Cardella, F. Hurd, C. Li, et al, “Design analysis and manufacturing of the cooling lines of the in vessel components of Wendelstein 7-X,” Fusion Engineering and Design, Vol 86, pp. 1669-1672, 2011.
- [3] B. Medevitch, A. Vorköper, J. Boscary, C. Li, N Dekorsy, A. Peacock, et al, “Lessons learned from the design and fabrication of the baffles and heat shields of Wendelstein 7-X,” Fusion Engineering and Design, Vol 86, pp. 1669-1672, 2011.
- [4] R. Tivey, T. Ando, A. Antipenkov, V. Barabash, S. Chiocchio, G. Federici, et al, “ITER divertor, design issues and research and development,” Fusion Engineering and Design, Vol 46, pp. 207-220, 1999.
- [5] T. Hirai, K. Ezato, and P. Majerus, “ITER relevant high heat flux testing on plasma facing surfaces,” Materials Transactions, Vol. 46, No. 3, pp. 412-424.
- [6] M. Richou, M. Missirlian, B. Riccardi, P. Gavila, C. Desgranges, N. Vignal, et al, “Assessment of CFC grades under thermal fatigue for the ITER inner vertical target,” Physica Scripta, Vol. T145, pp. 1-5, 2011.
- [7] J.D. Lore, T. Andreeva, J. Boscary, S. Bozhenkov, J. Geiger, J.H. Harris, et al, “Design and analysis of the divertor scraper elements for the W7-X stellarator,” submitted to IEEE Transactions on Plasma Science.
- [8] A. Lumsdaine, J. Tipton, J. Lore, D. McGinnis, J. Canik, J. Harris, et al, “Design and analysis of the W7-X divertor scraper element,” Fusion Engineering and Design, in press.
- [9] R.M. Manglik and A.E. Bergles, “Heat transfer and pressure drop correlations for twisted-tape inserts in isothermal tubes: part II – transition and turbulent flows,” J. Heat Transfer, Vol. 115, pp. 890-896, 1993.
- [10] H. Bas and V. Ozceyhan, “Heat transfer enhancement in a tube with twisted tape insters placed separately from the tube wall,” Experimental Thermal and Fluid Science, Vol. 41, pp. 51-58, 2012.
- [11] Flow of fluids through valves, fittings, and pipe, TP-410, Crane Co., Stamford, CT, (2009)
- [12] J.P. Bonal, “Thermal properties of carbon fiber composites before irradiation in Paride 3/4 experiment,” CEA, Direction des Reacteurs Nucleaires, Department de Mecanique et de Technologie (DMT), Report DMT SEMI/LM2E/RT2004.
- [13] H. Greuner, U. Toussaint, B. Böswirth, J. Boscary, and A. Peacock, “Results and consequences of high heat flux testing as quality assessment of the Wendelstein 7-X divertor,” Fusion Engineering and Design, in press.